

Electrical and Thermal Transport by Nodal Quasiparticles in the DDW State

Xiao Yang and Chetan Nayak

Physics Department, University of California, Los Angeles, CA 90095-1547

(November 3, 2018)

We compute the electrical and thermal conductivities and Hall conductivities of the d -density wave (DDW) state in the low-temperature impurity-scattering-dominated regime for low-dopings, at which they are dominated by nodal quasiparticles. We show that the longitudinal conductivity in this limit in the DDW state is not Drude-like. However, the thermal conductivity is Drude-like; this is a reflection of the discrepancy between electrical and thermal transport at finite frequency in the DDW state. An extreme example of this occurs in the $\mu = 0$, $\tau \rightarrow \infty$ limit, where there is a strong violation of the Wiedemann-Franz law: $\kappa_{xx}/\sigma_{xx} \propto T^2$ at $\omega = 0$ and $\kappa_{xx}/\sigma_{xx} = 0$ at finite frequency. The DDW electrical and thermal Hall conductivities are linear in the magnetic field, B , for weak fields. The formation of Landau levels at the nodes leads to the quantization of these Hall conductivities at high fields. In all of these ways, the quasiparticles of the DDW state differ from those of the $d_{x^2-y^2}$ superconducting (DSC) state.

PACS numbers: 71.10.Hf, 72.10.-d, 71.27.+a, 74.72-h

I. INTRODUCTION.

Transport measurements have produced a wealth of information about the high- T_c superconducting cuprates [1]. However, it is not immediately clear how this information can be used to shed light on their phase diagram. When inelastic processes determine transport coefficients, they are usually constrained by the very phase space restrictions which underlie Fermi liquid theory. Elastic scattering by impurities usually leads to a temperature- and frequency-independent scattering rate which is also not strongly dependent on the state of matter. Thus, transport coefficients need not bear a very strong imprint of the underlying phase. In more technical parlance, we would say that transport coefficients are usually determined by irrelevant operators, not by the fixed points themselves, except when they are determined by impurity scattering which drives most systems to a diffusive fixed point. However, the usual situation does not always hold, and in this paper we study one example where it does not. We show that the properties of nodal quasiparticles bespeak the broken symmetries which lead to their existence. Consequently, low-temperature transport in the highly underdoped limit (where it might be dominated by nodal excitations) can be used to reveal the physics of the pseudogap state of the underdoped cuprates.

In [2], it was proposed that the pseudogap phenomenon [3] in high- T_c cuprates is the result of the development of another order parameter called d -density wave order (DDW),

$$\langle c^{\alpha\dagger}(\mathbf{k} + \mathbf{Q}, t) c_{\beta}(\mathbf{k}, t) \rangle = i\Phi_{\mathbf{Q}} f(\mathbf{k}) \delta_{\beta}^{\alpha}, \quad (1)$$

where $f(\mathbf{k}) = \cos k_x a - \cos k_y a$. This order parameter breaks the symmetries of time-reversal, translation by one lattice spacing, and rotation by $\pi/2$, but respects the combination of any two of these. There is no modu-

lation of the charge density in this state since $f(\mathbf{k})$ vanishes upon integration about the Fermi surface. However, there are circulating currents in the ground state, which alternate from one plaquette to the next at wavevector $\mathbf{Q} = (\pi/a, \pi/a)$. The underdoped superconducting state was conjectured to exhibit both DDW order and $d_{x^2-y^2}$ superconducting (DSC) order. For hole dopings larger than a critical value $x_c \approx 0.19$, DDW order is presumed to disappear. The proposed phase diagram is indicated schematically in figure 1. As a result of its $d_{x^2-y^2}$ angular variation, DDW order bears some similarities to DSC order in its quasiparticle spectrum. However, as we show in this paper, the transport properties of these two phases are rather different.

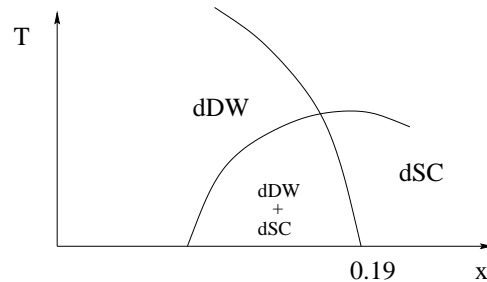


FIG. 1. Schematic proposed phase diagram for the cuprate superconductors.

The development of DDW order forms the basis for a compelling picture of the pseudogap because it qualitatively explains many of the hallmarks of pseudogap behavior such as the existence of a $d_{x^2-y^2}$ single-particle gap in photoemission [5,6] and tunneling [7], resonant inelastic neutron scattering (“the 41 meV peak”), c -axis transport [10], and the doping dependence of the superfluid density [11]. The basic physical picture underlying this description of the cuprates involves the interplay between two order parameters – one superconducting and

one density wave – similar to that observed in the A15 [12] and dichalcogenide [13,14] materials.

This consonance between theory and experiment is encouraging but far from conclusive. However, recent attempts to directly detect the DDW order parameter have the potential to be definitive. They have centered on the observation of the small magnetic fields ($\approx 10\text{G}$) which are generated by the circulating currents which appear to DDW order. *Elastic* neutron scattering experiments [15] on YBCO6.6 have found Bragg peaks in spin-flip scattering at wavevector $\mathbf{Q} = (\pi/a, \pi/a)$, with an onset temperature which is consistent with that determined by other probes of the pseudogap. These experiments thereby observe the symmetry-breaking pattern associated with DDW order. Antiferromagnetism also breaks time-reversal and translation by one lattice spacing, but the form factors measured in the experiment are more consistent with DDW order. A recent μSR experiment [16] finds evidence for small time-reversal symmetry breaking in YBCO. An exciting feature of these experiments is that the onset temperature is broadly consistent with the pseudogap scale in YBCO6.67 and the onset temperature is *below* T_c in YBCO6.95, as would be expected from a phase diagram of the type depicted in figure 1.

Can in-plane transport shed further light on the nature of the pseudogap state? In this paper, we show how nodal quasiparticles evince the symmetries of the phase which supports them by contrasting the transport properties of quasiparticles in the $d_{x^2-y^2}$ -density wave (DDW) and $d_{x^2-y^2}$ superconducting (DSC) phases. We show how the former reflect the broken translational symmetry of the DDW phase. We find a dichotomy between electrical and thermal transport; nodal quasiparticles in the DDW state carry electrical current much more effectively than they carry thermal current. A further distinction stems from the fact that the DDW state, unlike the DSC state, does not break gauge invariance, so the quasiparticles of the DDW state form Landau levels and have Hall electrical or thermal conductivities which are linear in the magnetic field, B , in contrast to their DSC cousins. These distinctions are sharpest in the limit of small μ , where the quasiparticle excitations of the DDW state are restricted to the vicinity of the nodal points. In this limit, the quasiparticles of the DDW state are analogous to ‘relativistic’ electrons and positrons. The quasiparticles of the DSC state, on the other hand, couple differently to the electromagnetic field as a result of their coherence factors which mix particle and hole states.

In section II, we briefly describe the low-energy effective field theories for quasiparticles in the DDW state, the DSC state, and the state with both DDW and DSC order. In section III, we use gauge invariance and Noether’s theorem to derive the electrical and energy current operators in these low-energy effective field theories. In sections IV and V, we present and discuss our results for

these conductivities in the three different phases considered. Finally, in section VI, we discuss our results and consider their possible range of validity. In appendix A, we discuss the Kubo formulae which relate the electrical and thermal conductivities and Hall conductivities to correlation functions of the appropriate current operators. In appendix B, we review impurity scattering of nodal quasiparticles.

II. NODAL QUASIPARTICLE HAMILTONIAN

The low-energy quasiparticle Hamiltonian for the DDW state is:

$$H^{\text{DDW}} = \int \frac{d^2k}{(2\pi)^2} [(\epsilon(k) - \mu) c^{\alpha\dagger}(k) c_\alpha(k) + i\Delta(k) c^{\alpha\dagger}(k) c_\alpha(k+Q)] \quad (2)$$

where $\epsilon(k)$ is the single-particle energy which we can, for instance, take to be

$$\epsilon(k) = -2t(\cos k_x a + \cos k_y a) + 4t' \cos k_x a \cos k_y a \quad (3)$$

while

$$\Delta(k) = \frac{\Delta_0}{2} (\cos k_x a - \cos k_y a) \quad (4)$$

is the d-wave order parameter of the DDW state. $\mathbf{Q} = (\frac{\pi}{a}, \frac{\pi}{a})$.

Since the order parameter breaks translational symmetry by one lattice spacing, it is convenient to halve the Brillouin zone and form a two-component electron operator:

$$\begin{pmatrix} \chi_{1\alpha} \\ \chi_{2\alpha} \end{pmatrix} = \begin{pmatrix} c_\alpha(k) \\ i c_\alpha(k+Q) \end{pmatrix} \quad (5)$$

Then the mean field Hamiltonian in terms of χ becomes

$$H = \int \frac{d^2k}{(2\pi)^2} \chi^{\alpha\dagger}(k) \left[\frac{1}{2}(\epsilon(k) + \epsilon(k+Q)) - \mu + \frac{1}{2}(\epsilon(k) - \epsilon(k+Q))\sigma^{(3)} + \Delta(k)\sigma^{(1)} \right] \chi_\alpha(k) \quad (6)$$

Where $\vec{\sigma}$ are Pauli matrices which mix the two translational components of (5).

The single-quasiparticle energy is:

$$E_\pm(k) = \frac{1}{2}(\epsilon(k) + \epsilon(k+Q)) \pm \frac{1}{2}\sqrt{(\epsilon(k) - \epsilon(k+Q))^2 + 4\Delta^2(k)} \quad (7)$$

At exactly half-filling, there are 4 nodal points ($\pm\frac{\pi}{2a}, \pm\frac{\pi}{2a}$) at which there are gapless excitations. In the vicinity of these ‘Dirac points’, the spectrum is conical. When the chemical potential is less than 0, the states will be filled up to $E_-(k) = \mu$, so the nodes will

open into small pockets which are cross sections of the ‘Dirac cone’. The low-energy physics will be dominated by these gapless fermionic excitations. We can focus on a single pair of nodal points, $(\frac{\pi}{2a}, \frac{\pi}{2a})$ and $(-\frac{\pi}{2a}, -\frac{\pi}{2a})$. It is straightforward to include the other pair of nodes into our result at the end of any calculation. We choose the x-axis to be perpendicular to the free-electron Fermi surface and the y-axis to be parallel to the free-electron Fermi surface at one antipodal pair of nodes; the x-axis is parallel to the free-electron Fermi surface and the y-axis is perpendicular to the free-electron Fermi surface at the other pair.

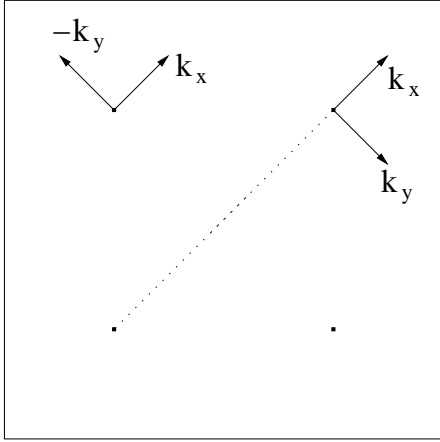


FIG. 2. The quasiparticle spectra are linearized about the Fermi points $(\pm\pi/2, \pm\pi/2)$. We choose the x and y axes as shown. Each pair of antipodal nodes (shown connected by dotted lines) is combined to form a single Dirac fermion.

Linearizing the spectrum about the nodes, we obtain the linearized dispersion relation:

$$E(k) = \pm \sqrt{v_F^2 k_x^2 + v_{\Delta}^{\text{DDW}} k_y^2} \quad (8)$$

where $v_F = 2\sqrt{2}ta$ and $v_{\Delta}^{\text{DDW}} = \sqrt{2}\Delta_0 a$; t' does not enter at linear order. The effective Lagrangian of the nodal quasiparticles is:

$$\mathcal{L}_{eff}^{\text{DDW}} = \chi_{\alpha}^{1\dagger} (\partial_{\tau} + \mu - v_F \sigma^{(3)} i \partial_x - v_{\Delta}^{\text{DDW}} \sigma^{(1)} i \partial_y) \chi_{\alpha}^1 + \chi_{\alpha}^{2\dagger} (\partial_{\tau} + \mu - v_{\Delta}^{\text{DDW}} \sigma^{(3)} i \partial_x - v_F \sigma^{(1)} i \partial_y) \chi_{\alpha}^2 \quad (9)$$

The superscript 1,2 labels the two antipodal pairs of nodal points. Note that the chemical potential, μ , moves the free-electron Fermi surface away from the nodes and opens Fermi pockets which are the sections of the Dirac cone referred to earlier. When μ is small, the Fermi surface will remain in the vicinity of the nodes and we can use the linearized effective action (9). In this paper, we will work in the linearized approximation; in the discussion, we will examine the regime of validity of this approximation. The associated nodal quasiparticle Green functions are

$$G^1(i\epsilon_n, \mathbf{k}) = \frac{i\epsilon_n + \mu + \sigma_z v_F k_x + \sigma_x v_{\Delta}^{\text{DDW}} k_y}{(i\epsilon_n + \mu)^2 - v_F^2 k_x^2 - (v_{\Delta}^{\text{DDW}})^2 k_y^2} \quad (10)$$

and a similar expression for $G^2(i\epsilon_n, \mathbf{k})$ with v_F and v_{Δ}^{DDW} exchanged.

Now consider the DSC state. We can write the low-energy quasiparticle Hamiltonian as:

$$H^{\text{DSC}} = \int \frac{d^2k}{(2\pi)^2} \psi_{\alpha}^{\dagger}(k) \left[\tau^{(3)} (\epsilon(\mathbf{k}) - \mu) + \tau^{(1)} \Delta(k) \right] \psi_{\alpha}(k) \quad (11)$$

where

$$\begin{bmatrix} \psi_{1\alpha}(\vec{k}) \\ \psi_{2\alpha}(\vec{k}) \end{bmatrix} = \begin{bmatrix} c_{k\alpha} \\ \epsilon_{\alpha\beta} c_{-k\beta}^{\dagger} \end{bmatrix}. \quad (12)$$

and the Pauli matrices τ act on the particle-hole indices of this Nambu-Gorkov spinor.

We now linearize the spectrum about $(\pm\frac{\pi}{2a}, \pm\frac{\pi}{2a})$, which is not the same as linearizing about the free-electron Fermi surface $\epsilon(k) = \mu$ (which is more conventional) if $\mu \neq 0$. We obtain the effective action for DSC quasiparticles:

$$\mathcal{L}_{eff}^{\text{DSC}} = \psi_{\alpha}^{1\dagger} (\partial_{\tau} - v_F \tau^{(3)} (i \partial_x - \mu) - v_{\Delta}^{\text{DSC}} \tau^{(1)} i \partial_y) \psi_{\alpha}^1 + (1 \rightarrow 2, x \leftrightarrow y) \quad (13)$$

Again, the superscript 1,2 labels the pairs of nodes. The Green functions are formally similar, although the matrix labels have different meanings; they label magnetic zones in the DDW case and they label particles and holes in the DSC case. An important difference between the two states is that in the DSC case, the chemical potential moves the nodes along with the Fermi surface so that they are at $k_x = \mu/v_F$.

The difference in the way in which the chemical potential, μ , enters the DDW and DSC nodal quasiparticle Hamiltonians is a harbinger of the difference in their electrical responses. In the next section, we show how this difference manifests itself in the form of the current operators in the two states.

First, however, let us consider a state with both order parameters. It is useful to define a four-component object, Ψ :

$$\begin{pmatrix} \Psi_1 \\ \Psi_2 \\ \Psi_3 \\ \Psi_4 \end{pmatrix} = \begin{pmatrix} c_{\alpha}(k) \\ c_{\alpha}(k+Q) \\ \epsilon_{\alpha\beta} c_{\beta}^{\dagger}(-k) \\ \epsilon_{\alpha\beta} c_{\beta}^{\dagger}(-k-Q) \end{pmatrix}$$

Linearizing about the nodal points at half-filling, $(\pm\frac{\pi}{2a}, \pm\frac{\pi}{2a})$, we can write the effective action as:

$$\mathcal{L}_{eff}^{\text{DDW}+\text{DSC}} = \Psi^{\dagger} \left(\partial_{\tau} + \mu \Gamma^c - v_F \Gamma^1 i \partial_x - v_{\Delta}^{\text{DSC}} \Gamma^2 i \partial_y - v_{\Delta}^{\text{DDW}} \Gamma^3 i \partial_y \right) \Psi \quad (14)$$

where

$$\begin{aligned}\Gamma^c &= \begin{pmatrix} I & 0 \\ 0 & -I \end{pmatrix} \\ \Gamma^1 &= \begin{pmatrix} \sigma^3 & 0 \\ 0 & -\sigma^3 \end{pmatrix} \\ \Gamma^2 &= \begin{pmatrix} 0 & \sigma^1 \\ \sigma^1 & 0 \end{pmatrix} \\ \Gamma^3 &= \begin{pmatrix} \sigma^2 & 0 \\ 0 & -\sigma^2 \end{pmatrix}\end{aligned}$$

III. ELECTRICAL AND ENERGY CURRENT OPERATORS

Although the DSC and DDW states have similar quasiparticle spectra near their nodal points, the coupling of these quasiparticles to the electromagnetic field is different. As a result, the electrical current operators are different in the two states.

In the DSC state, the electrical current is:

$$\begin{aligned}j_x &= -ev_F \psi_\alpha^{1\dagger} \psi_\alpha^1 \\ j_y &= ev_F \psi_\alpha^{2\dagger} \psi_\alpha^2\end{aligned}\quad (15)$$

At a given node, there is no current parallel to the Fermi surface; hence, there is no contribution of ψ_α^1 to j_y and no contribution of ψ_α^2 to j_x . In essence, the DSC order parameter does not affect the quasiparticle current.

In the DDW state, the electrical current is given by

$$\begin{aligned}j_x &= -ev_F \chi_\alpha^{1\dagger} \sigma^{(3)} \chi_\alpha^1 + ev_\Delta \chi_\alpha^{2\dagger} r_\alpha \sigma^{(1)} \chi_\alpha^2 \\ j_y &= -ev_\Delta \chi_\alpha^{1\dagger} \sigma^{(1)} \chi_\alpha^1 + ev_F \chi_\alpha^{1\dagger} \sigma^{(3)} \chi_\alpha^1\end{aligned}\quad (16)$$

Both nodes contribute to the current operators in both directions. As a result of the DDW order parameter, the quasiparticle current operator is modified from its free-particle form.

However, the energy current operator is identical in form in the two states:

$$\begin{aligned}j_x^E &= \frac{i}{2} v_F (\chi^{1\dagger} \sigma^{(3)} \dot{\chi}^1 - h.c.) - \frac{i}{2} v_\Delta (\chi^{2\dagger} \sigma^{(1)} \dot{\chi}^2 - h.c.) \\ j_y^E &= \frac{i}{2} v_\Delta (\chi^{1\dagger} \sigma^{(1)} \dot{\chi}^1 - h.c.) - \frac{i}{2} v_F (\chi^{2\dagger} \sigma^{(3)} \dot{\chi}^2 - h.c.)\end{aligned}\quad (17)$$

where v_Δ is either v_Δ^{DDW} or v_Δ^{DSC} and χ is replaced by ψ in the latter case.

To see how (15)-(17) arise, first consider the quasiparticle ‘‘kinetic energy’’ in the DSC state:

$$H_{DSC} = \int d^2x \psi^\dagger v_F \tau^{(3)} (i\partial_x - \mu) \psi +$$

$$\int d^2x d^2x' \Delta^{\text{DSC}}(R, x - x') \psi^\dagger(x) \tau^{(1)} \psi(x') \quad (18)$$

In the second line, we have written the gap, Δ^{DSC} , which is a function of the two electron coordinates, x and x' , in terms of the center-of-mass coordinate, R , and the relative coordinate, $x - x'$. The $\tau^{(i)}$ are Pauli matrices.

We should insert the electromagnetic field into this Hamiltonian in order to make it invariant under the gauge transformation

$$\begin{aligned}\psi &\rightarrow e^{i\tau^{(3)}\varphi(x)} \psi \\ \Delta^{\text{DSC}}(R, x - x') &\rightarrow e^{-2i\varphi(R)} \Delta^{\text{DSC}}(R, x - x')\end{aligned}\quad (19)$$

The second line of (19) is accurate to lowest order in $x - x'$, which is sufficient since we will eventually be linearizing about the nodes. The first line of (19) includes both of the transformation laws

$$\begin{aligned}c_\alpha(x) &\rightarrow e^{i\varphi(x)} c_\alpha(x) \\ c_\alpha^\dagger(x) &\rightarrow e^{-i\varphi(x)} c_\alpha^\dagger(x)\end{aligned}\quad (20)$$

The dependence of the gap on $x - x'$ determines the structure of the pair wavefunction. In a d -wave superconductor the two electrons in a pair cannot be on the same site. For instance, if the gap varies as $\cos k_x a - \cos k_y a$, the distance between the electrons, or the pair size, is one lattice constant. When we linearize the gap about the nodes, we treat this pair size as if it were infinitesimal. In order to see how this works, let us, as in the previous section, align the axes so that the x -axis is perpendicular to the Fermi surface and the y -axis is parallel to the Fermi surface. Let us assume that the pairs have a fixed size a and that they are oriented along the \hat{y} axis. Then, we linearize the gap by making the following approximation:

$$\begin{aligned}\Delta^{\text{DSC}}(\mathbf{R}, \mathbf{x} - \mathbf{x}') &= \\ v_\Delta(\mathbf{R}) \left(\frac{i}{2a} \right) [\delta(\mathbf{x} - \mathbf{x}' + a\hat{y}) - \delta(\mathbf{x} - \mathbf{x}' - a\hat{y})] \\ &\approx v_\Delta(\mathbf{R}) \Delta^{\text{DSC}}(\mathbf{R}) i\partial_y\end{aligned}\quad (21)$$

Under a gauge transformation, the gap transforms as

$$\begin{aligned}v_\Delta(\mathbf{R}) \left(\frac{i}{2a} \right) [\delta(\mathbf{x} - \mathbf{x}' + a\hat{y}) - \delta(\mathbf{x} - \mathbf{x}' - a\hat{y})] \\ \rightarrow e^{-2i\varphi(\mathbf{R})} v_\Delta(\mathbf{R}) \left(\frac{i}{2a} \right) \left[\delta(\mathbf{x} - \mathbf{x}' + a\hat{y}) - \delta(\mathbf{x} - \mathbf{x}' - a\hat{y}) \right] \\ = v_\Delta(\mathbf{R}) \left(\frac{i}{2a} \right) \left[e^{-2i\varphi(\mathbf{x} + \frac{a}{2}\hat{y})} \delta(\mathbf{x} - \mathbf{x}' + a\hat{y}) - e^{-2i\varphi(\mathbf{x} - \frac{a}{2}\hat{y})} \delta(\mathbf{x} - \mathbf{x}' - a\hat{y}) \right] \\ \approx v_\Delta(\mathbf{R}) \delta(\mathbf{x} - \mathbf{x}') \frac{1}{2} i\partial_y e^{-2i\varphi(\mathbf{x})} \\ \approx v_\Delta(\mathbf{R}) \delta(\mathbf{x} - \mathbf{x}') e^{-i\varphi(\mathbf{x})} i\partial_y e^{-i\varphi(\mathbf{x})}\end{aligned}\quad (22)$$

In other words, if we linearize the Hamiltonian about the nodes, as in the previous section,

$$H_{DSC} = \int d^2x \psi^\dagger v_F \tau^{(3)} (i\partial_x - \mu) \psi + \int d^2x \psi^\dagger v_\Delta^{\text{DSC}} \tau^{(1)} i\partial_y \psi \quad (23)$$

then the gap transforms as

$$v_\Delta i\partial_y \rightarrow v_\Delta e^{-i\varphi(\mathbf{x})} i\partial_y e^{-i\varphi(\mathbf{x})} \quad (24)$$

Hence, the second (gap) term in the Hamiltonian is already gauge-invariant, even without inserting the electromagnetic field. In order to make the Hamiltonian gauge-invariant, we must couple the electromagnetic field in the following way:

$$H_{DSC} = \int d^2x \psi^\dagger v_F \tau^{(3)} (i\partial_x + eA_x \tau^{(3)} - \mu) \psi + \int d^2x \psi^\dagger v_\Delta^{\text{DSC}} \tau^{(1)} i\partial_y \psi \quad (25)$$

Consequently,

$$\begin{aligned} j_x &= -ev_F \psi^\dagger \psi_{\alpha A} \\ j_y &= 0 \end{aligned} \quad (26)$$

in the DSC state. Combining this with the contribution from the other set of nodes, we obtain (15).

Now consider the DDW effective Hamiltonian:

$$H_{\text{DDW}} = \int d^2x \chi_{\alpha A}^\dagger \sigma_{AB}^{(3)} v_F i\partial_x \chi_{\alpha A} + \int d^2x d^2x' \Delta^{\text{DDW}}(R, x - x') \chi_{\alpha A}^\dagger \sigma_{AB}^{(1)} \chi_{\alpha B} \quad (27)$$

The $\sigma^{(i)}$ are Pauli matrices. We want this effective Hamiltonian to be invariant under

$$\begin{aligned} \chi_{\alpha A} &\rightarrow e^{i\varphi(x)} \chi_{\alpha A} \\ \chi_{\alpha A}^\dagger &\rightarrow e^{-i\varphi(x)} \chi_{\alpha A}^\dagger \\ \Delta^{\text{DDW}}(R, x - x') &\rightarrow \Delta^{\text{DDW}}(R, x - x') \end{aligned} \quad (28)$$

The third line of (28) is accurate to lowest order in $x - x'$, which is sufficient since we will linearize about the nodes:

$$\Delta^{\text{DDW}}(R, x - x') \approx v_\Delta \delta(\mathbf{x} - \mathbf{x}') i\partial_y \quad (29)$$

Both terms in the linearized Hamiltonian

$$H_{\text{DDW}} = \int d^2x \chi_{\alpha A}^\dagger \sigma_{AB}^{(3)} v_F i\partial_x \chi_{\alpha A} + \chi_{\alpha A}^\dagger \sigma_{AB}^{(1)} v_\Delta i\partial_y \chi_{\alpha A} \quad (30)$$

transform under a gauge transformation, so the electromagnetic field must be inserted in both terms in the linearized Hamiltonian

$$H_{\text{DDW}} = \int d^2x \chi_{\alpha A}^\dagger \sigma_{AB}^{(3)} v_F (i\partial_x + eA_x) \chi_{\alpha A} +$$

$$\int d^2x \chi_{\alpha A}^\dagger \sigma_{AB}^{(1)} v_\Delta (i\partial_y + eA_y) \chi_{\alpha A} \quad (31)$$

Hence, the current operator in the DDW state takes the form

$$\begin{aligned} j_x &= -ev_F \chi_{\alpha A}^\dagger \sigma_{AB}^{(3)} \chi_{\alpha B} \\ j_y &= -ev_\Delta \chi_{\alpha A}^\dagger \sigma_{AB}^{(1)} \chi_{\alpha B} \end{aligned} \quad (32)$$

Combining this with the contribution from the other node, we obtain (16).

Now consider the state with both DDW and DSC order. Its quasiparticles have effective action:

$$\begin{aligned} \mathcal{L}_{eff}^{\text{DDW+DSC}} &= \Psi^\dagger \left(\partial_\tau + \mu \Gamma^\mu - v_F \Gamma^1 i\partial_x \right. \\ &\quad \left. - v_\Delta^{\text{DSC}} \Gamma^2 i\partial_y - v_\Delta^{\text{DDW}} \Gamma^3 i\partial_y \right) \Psi \end{aligned} \quad (33)$$

From the preceding discussion of the two order parameters separately, it is clear that the correct minimally-coupled form of the action is:

$$\begin{aligned} \mathcal{L}_{eff}^{\text{DDW+DSC}} &= \Psi^\dagger \left(\partial_\tau + \mu \Gamma^c - v_F \Gamma^1 (i\partial_x + eA_x \Gamma^c) \right. \\ &\quad \left. - v_\Delta^{\text{DSC}} \Gamma^2 i\partial_y - v_\Delta^{\text{DDW}} \Gamma^3 (i\partial_y + eA_y \Gamma^c) \right) \Psi \end{aligned} \quad (34)$$

from which it follows that the electrical current is given by:

$$\begin{aligned} j_x &= -ev_F \Psi^\dagger \Gamma^1 \Gamma^c \Psi \\ j_y &= -ev_\Delta^{\text{DDW}} \Psi^\dagger \Gamma^3 \Gamma^c \Psi \end{aligned} \quad (35)$$

In order to compute the thermal conductivity, we will need the heat current. The heat current j^Q is related to the energy current j^E and the electrical current j according to:

$$\mathbf{j}^Q = \mathbf{j}^E - \frac{\mu}{e} \mathbf{j} \quad (36)$$

The thermal conductivity is measured under a condition of vanishing electrical current flow, $\mathbf{j} = 0$, so that $\mathbf{j}^Q = \mathbf{j}^E$. The energy current may be obtained from Noether's theorem. It is given by off-diagonal components of the energy-momentum tensor:

$$j_i^E = T_{0i} = \pi_i \partial_0 \phi + \pi_i^\dagger \partial_0 \phi^\dagger \quad (37)$$

where ϕ and ϕ^\dagger are the basic fields in the theory and $\pi_i = \partial \mathcal{L} / \partial (\partial_i \phi)$ are their canonical conjugates. (Note that T_{i0} is the momentum density, which can be distinct from T_{0i} , the energy current.)

In the DDW phase, this is:

$$\begin{aligned} j_x^E &= \frac{i}{2} v_F (\chi^\dagger \sigma^{(3)} \dot{\chi} - h.c) \\ j_y^E &= \frac{i}{2} v_\Delta^{\text{DDW}} (\chi^\dagger \sigma^{(1)} \dot{\chi} - h.c) \end{aligned} \quad (38)$$

while, in the DSC phase, it is identical in form:

$$\begin{aligned} j_x^E &= \frac{i}{2} v_F (\psi^\dagger \tau^{(3)} \dot{\psi} - h.c) \\ j_y^E &= \frac{i}{2} v_\Delta^{\text{DSC}} (\psi^\dagger \tau^{(1)} \dot{\psi} - h.c) \end{aligned} \quad (39)$$

When both order parameters are present, the energy current is given by

$$\begin{aligned} j_x^E &= \frac{i}{2} v_F (\Psi^\dagger \Gamma^1 \dot{\Psi} - h.c) \\ j_y^E &= \frac{i}{2} \left(\psi^\dagger (v_\Delta^{\text{DSC}} \Gamma^2 + v_\Delta^{\text{DDW}} \Gamma^3) \dot{\psi} - h.c \right) \end{aligned} \quad (40)$$

We can use these current operators and the Green functions derived in the previous section or in appendix B to compute electrical and thermal conductivities according to the Kubo formulae given in appendix A. In the next section, we will do this in the clean limit in which there are no impurities. In section V, we will consider the more realistic case in which the nodal quasiparticles have a finite lifetime as a result of impurity scattering.

IV. ELECTRICAL AND THERMAL CONDUCTIVITIES IN THE CLEAN LIMIT

A. DDW State

It is instructive to consider the electrical and thermal conductivities of the DDW state in the simplest case imaginable: a completely pure system with no impurities and no phonons. Let us further neglect all interactions between the nodal quasiparticles. Eventually, we will restore impurity scattering and consider the low-temperature limit in which impurity scattering dominates. However, it is instructive to consider the ideal case first.

The frequency- and temperature-dependent electrical conductivity consists of *two* contributions:

$$\sigma_{xx}(\omega, T) = \sigma_{xx}^{\text{Drude}}(\omega, T) + \sigma_{xx}^{\text{Inter}}(\omega, T) \quad (41)$$

The appellations ‘Drude’ and ‘Inter’ will be explained shortly. These contributions have the form

$$\sigma_{xx}^{\text{Drude}}(\omega, T) = \frac{1}{2} e^2 \alpha \delta(\omega) \left[\int_{-\infty}^{\infty} dx \frac{|\mu + xT| e^x}{(e^x + 1)^2} \right] \quad (42)$$

$$\sigma_{xx}^{\text{Inter}}(\omega, T) = \frac{1}{8} e^2 \alpha \left| n_F \left(-\frac{\omega}{2} - \mu \right) - n_F \left(\frac{\omega}{2} - \mu \right) \right|$$

where

$$\alpha = \frac{v_F}{v_\Delta^{\text{DDW}}} + \frac{v_\Delta^{\text{DDW}}}{v_F} \quad (43)$$

In the zero-temperature limit, this is

$$\begin{aligned} \sigma_{xx}^{\text{Drude}}(\omega, 0) &= \frac{1}{2} e^2 \alpha |\mu| \delta(\omega) \\ \sigma_{xx}^{\text{Inter}}(\omega, 0) &= \frac{1}{8} e^2 \alpha \theta \left(\left| \frac{\omega}{2} \right| - |\mu| \right) \end{aligned} \quad (44)$$

The first contribution, $\sigma_{xx}^{\text{Drude}}(\omega, T)$, to the conductivity is Drude-like: it is proportional to a δ -function in frequency multiplied by the density of states at the Fermi level. As in an ordinary Fermi gas, a uniform electric field can excite a particle-hole pair of momentum $\mathbf{q} = 0$, which, at $T = 0$, must be precisely at the Fermi surface. However, the second term, $\sigma_{xx}^{\text{Inter}}(\omega, T)$, is special to a Dirac cone: a uniform, finite-frequency electric field can excite a quasiparticle from a state of energy $-\epsilon$ to a state of energy ϵ at the same momentum. There is no gap in the spectrum, so such particle-hole pairs can be created all the way down to $|\omega| = 2|\mu|$. The existence of this term follows from both translational symmetry-breaking and rotational symmetry-breaking. In a crystalline solid, there will always be, in addition to the usual Drude term, contributions to the conductivity resulting from interband transitions. However, these will be at frequencies higher than the band gap. In the case of the DDW state, the DDW ‘band’ gap vanishes at the nodal points as a result of the $d_{x^2-y^2}$ order parameter symmetry which breaks rotational symmetry, so ‘Interband’ transitions contribute to the conductivity to arbitrarily low frequencies at $\mu = 0$.

Note that at $\mu = 0$, the Drude contribution vanishes linearly with temperature, and the Interband contribution dominates the conductivity

$$\begin{aligned} \sigma_{xx}^{\mu=0}(\omega, T) &= \frac{1}{8} e^2 \alpha \left| n_F \left(-\frac{\omega}{2} \right) - n_F \left(\frac{\omega}{2} \right) \right| \\ &\quad + (\ln 2) e^2 \alpha T \delta(\omega) \end{aligned} \quad (45)$$

The Interband contribution extends to zero frequency and yields a DC conductivity $e^2 \alpha / 8$ at $T = 0$.

Let us now consider the thermal conductivity in the same ideal situation. The thermal current is not proportional to the momentum even in a Galilean-invariant system [17], so there could be a non-Drude contribution – i.e. one which is not proportional to $\delta(\omega)$ – even in the absence of translational symmetry-breaking. In the DDW state, this contribution results from the same excitations which lead to $\sigma_{xx}^{\text{Inter}}(\omega, T)$, so we will use the same moniker.

$$\kappa_{xx}(\omega, T) = \kappa_{xx}^{\text{Drude}}(\omega, T) + \kappa_{xx}^{\text{Inter}}(\omega, T) \quad (46)$$

with

$$\begin{aligned} \kappa_{xx}^{\text{Drude}}(\omega, T) &= \frac{1}{2} \alpha T \delta(\omega) \left[\int_{-\infty}^{\infty} dx |\mu + xT| \frac{x^2 e^x}{(e^x + 1)^2} \right] \\ \kappa_{xx}^{\text{Inter}}(\omega, T) &= \frac{1}{4T} \alpha \mu^2 \left| n_F \left(-\frac{\omega}{2} - \mu \right) - n_F \left(\frac{\omega}{2} - \mu \right) \right| \end{aligned} \quad (47)$$

At $\mu = 0$, the Interband contribution vanishes and the Drude contribution is proportional to T^2 :

$$\kappa_{xx}^{\mu=0}(\omega, T) = \frac{9}{2} \zeta(3) \alpha T^2 \delta(\omega) \quad (48)$$

Note that this strongly violates the Wiedemann-Franz law because σ and κ/T have entirely different temperature dependences since the former has an Interband part but the latter does not.

This violation of the Wiedemann-Franz law can be understood in the following terms. At $\mu = 0$, Interband excitations create a quasihole in a negative energy state of energy $-E_k$ – therefore costing positive energy E_k – and create a quasiparticle in a positive energy state with energy $E_k = -E_k + \omega$. The quasiparticle and quasihole states have opposite momenta (since the quasihole is the absence of a particle at \mathbf{k}) and carry opposite charge. Hence, the resulting state carries current proportional to $e\mathbf{k} + (-e)(-\mathbf{k}) = 2e\mathbf{k}$. However, the two states carry the same energy, $E_k = \omega/2$, so the energy current is $E_k\mathbf{k} + E_k(-\mathbf{k}) = 0$. Put more simply, the violation of the Wiedemann-Franz law is due to the ‘relativistic’ spectrum of the nodal quasiparticles. If we were to imagine creating an electron-positron pair with total momentum zero, we would have the same situation.

For $|\mu| > T$, the Drude contribution is:

$$\kappa_{xx}^{\text{Drude}}(\omega, T) = \frac{\pi^2}{6} |\mu| T \delta(\omega) \quad (49)$$

If $|\mu| < T$, the $\mu = 0$ result is recovered. For $|\omega| \ll |\mu|$, the Interband contribution is

$$\kappa_{xx}^{\text{Inter}}(\omega, T) = \frac{\mu^2 \alpha \omega}{16T^2 \cosh^2(\frac{\mu}{2T})} \sim \frac{1}{T^2} e^{-\mu/2T} \quad (50)$$

If we try to take $\omega > T$, we will encounter pathological results, which are related to heating. In order to obtain sensible answers, we must include electron-phonon interactions or some other mechanism by which equilibrium can be maintained. This is analogous to the divergence which arises in the non-linear response to an electric field [19]. However, we can consider the limit $\mu \ll \omega \ll T$, where:

$$\kappa_{xx}^{\text{Inter}}(\omega, T) = \frac{\mu^2 \alpha}{4T} \left| \tanh \frac{\omega}{4T} \right| \quad (51)$$

Thus, to summarize, we see that, in the limit of a perfectly clean DDW state, there is no Wiedemann-Franz law relating $\kappa_{xx}^{\text{Inter}}(\omega, T)$ and $\sigma_{xx}^{\text{Inter}}(\omega, T)$. Instead,

$$\kappa_{xx}^{\text{Inter}}(\omega, T) = \frac{2\mu^2}{e^2 T} \sigma_{xx}^{\text{Inter}}(\omega, T) \quad (52)$$

Meanwhile, there is a Wiedemann-Franz law for $\kappa_{xx}^{\text{Drude}}(\omega, T)$ and $\sigma_{xx}^{\text{Drude}}(\omega, T)$.

$$\frac{1}{T} \kappa_{xx}^{\text{Drude}}(\omega, T) = \frac{L}{e^2} \sigma_{xx}^{\text{Drude}}(\omega, T) \quad (53)$$

where $L = \pi^2/3$ for $|\mu| > T$ and $L = 9\zeta(3)/(2\ln 2)$ for $|\mu| < T$.

B. DSC State

Let us now consider the same quantities in the DSC state. Because DSC order does not break translational symmetry, we do not expect to have an Interband contribution. Furthermore, we might expect the Drude contribution to vanish at $T = 0$ because the chemical potential merely moves the Dirac points, it does not open Fermi pockets, unlike in the case of the DDW state. This is confirmed by a direct calculation:

$$\sigma_{xx}^{\text{qp}}(\omega, T) = (\ln 2) e^2 \left(\frac{v_F}{v_{\Delta}^{\text{DSC}}} \right) T \quad (54)$$

At a calculational level, there is a difference between the DSC case and the $\mu = 0$ DDW case resulting from the absence of a $\tau^{(3)}$ Pauli matrix in the current operator in the direction perpendicular to the bare Fermi surface in the DSC case. Furthermore, the current operator in the direction parallel to the Fermi surface vanishes in the DSC state. This is a reflection of the coherence factors of the superconducting state; a quasiparticle is a superposition of an electron and a hole which becomes neutral in the limit that the Fermi surface is approached.

Of course, the superconducting condensate carries electrical current in the DSC state, so (54) does not imply that the state is an electrical insulator. Note that nodal quasiparticles reduce the superfluid density in the clean limit, but this must be obtained from a somewhat different calculation since the superfluid density is obtained from a different order of limits of the current-current correlation [18].

The thermal conductivity calculation in the DSC state is identical to that in the DDW state, with v_{Δ}^{DDW} replaced by v_{Δ}^{DSC} , as may be seen from the formal identity between (38) and (39).

Thus, we see that, in the clean limit, the quasiparticles of the DDW and DSC states are very different in their transport properties despite the similarity in their spectra. DDW quasiparticles carry electrical current but negligible thermal current in the small μ limit. Even for larger values of μ , the disparity between electrical and thermal transport can be seen at finite frequency, where $\kappa_{xx}^{\text{Inter}}(\omega, T) \ll T \sigma_{xx}^{\text{Inter}}(\omega, T)$. On the other hand, the quasiparticles of the DSC state are able to carry electrical and thermal currents with essentially equal facility or lack thereof.

C. Simultaneous DDW and DSC Order

Finally, we consider a state with simultaneous DDW and DSC order. The result for the electrical conductivity is the same as in a state with DDW order alone, but with

a modified α :

$$\alpha \rightarrow \frac{1}{\sqrt{(v_{\Delta}^{\text{DDW}})^2 + (v_{\Delta}^{\text{DSC}})^2}} \left(v_F + \frac{(v_{\Delta}^{\text{DDW}})^2}{v_F} \right) \quad (55)$$

The conductivity has both Drude and Interband components because translational symmetry is broken by the DDW order parameter. The density-of-states is decreased by the development of DSC order, and the conductivity is decreased by this factor.

The thermal conductivity is the same as in the DDW or DSC state, but with v_{Δ}^{DDW} or v_{Δ}^{DSC} replaced by:

$$v_{\Delta}^{\text{DDW}}, v_{\Delta}^{\text{DSC}} \rightarrow \sqrt{(v_{\Delta}^{\text{DDW}})^2 + (v_{\Delta}^{\text{DSC}})^2} \quad (56)$$

V. ELECTRICAL AND THERMAL CONDUCTIVITIES IN THE IMPURITY-SCATTERING-DOMINATED LIMIT

Now consider the more realistic situation in which the quasiparticles of the DDW state have finite lifetimes as a result of impurity scattering. We will continue to neglect the effects of quasiparticle-quasiparticle scattering, which is irrelevant in the low-frequency, low-temperature limit. (The primary effect of electron-electron interactions is, thus, assumed to be the formation of the DDW state; the residual interactions can be neglected in the low-energy limit.) The basic effect of impurity scattering is to smear out momenta so that $E(k)$ has an uncertainty $1/\tau$. As a result, the frequency dependence of our expressions for the electrical and thermal conductivity are essentially convoluted with a Lorentzian in frequency of width $1/\tau$. Thus, for instance, $\delta(\omega)$ is replaced by $(\tau/\pi)/(1 + \omega^2\tau^2)$. Furthermore, we expect that μ will be replaced by a function which behaves like $\max(\mu, 1/2\tau)$. Note that when τ is finite, there is no longer a sharp separation between the Drude and Interband components of the conductivity. Nevertheless, we will still use this terminology since, as a practical matter, we can decompose the conductivity into the impurity-broadened versions of the two components of the clean limit.

Consider the DC conductivity of the DDW state for $\mu = 0$:

$$\begin{aligned} \sigma_{xx}^{\text{DC}}(0, T) &= 2\pi \int \frac{d^2k}{(2\pi)^2} \text{Tr} \left\{ A^B(k, 0) \tau^{(3)} A^B(k, 0) \tau^{(3)} \right\} \\ &= \frac{e^2}{2\pi^2} \alpha \end{aligned} \quad (57)$$

From the expression for $A(k, 0)$ given in the appendix, we see that it is proportional to the identity matrix. Hence, the $\tau^{(3)}$ s have no effect. As a result, the DC conductivity of quasiparticles in the DSC state follows from an identical calculation, with v_{Δ}^{DDW} replaced by v_{Δ}^{DSC} but there

is only a contribution from the single pair of nodes at which $j_x \neq 0$ in the DDW state:

$$\sigma_{xx}^{\text{DC}}(0, T) = \frac{e^2}{2\pi^2} \frac{v_F}{v_{\Delta}^{\text{DSC}}} \quad (58)$$

As we discussed above, the Drude contribution to the conductivity is modified by two effects: the Dirac points are broadened and acquire a width $1/\tau$; and the δ -function is broadened into a Lorentzian with zero-frequency height τ . The τ -dependence cancels, so the Drude term in the conductivity is independent of τ .

Now consider the DDW state for finite μ . If $|\mu| > 1/\tau$, the conductivity in the zero-temperature DC limit is

$$\sigma_{xx}^{\text{Drude}}(0, 0) = \frac{1}{4\pi} e^2 \alpha |\mu| \tau \quad (59)$$

There is only a Drude component in this limit.

Now let us consider the Interband conductivity for finite τ . The DSC state has no such contribution, whether or not τ is finite. Hence, we consider the DDW state only. The Interband contribution is qualitatively the same as in the clean limit, but now smeared on a frequency scale $1/\tau$, as may be seen from the plot of conductivity vs. frequency in Fig. 3

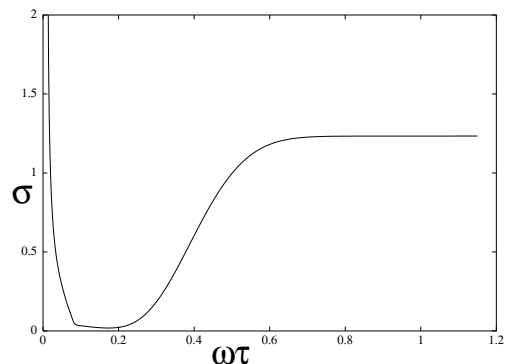


FIG. 3. The frequency-dependent conductivity of the DDW state in the impurity-scattering-dominated limit. The conductivity is in units of $8/e^2\alpha$ while the scale for $\omega\tau$ is 10^{-4} .

The thermal conductivity is formally identical in the DSC state and the DDW state at $\mu = 0$. The Drude contribution is:

$$\kappa_{xx}^{\text{Drude}}(0, T \rightarrow 0) = \frac{1}{6} \alpha T \quad (60)$$

where α is understood to be the expression in (43) or its analogue for the DSC state.

The Interband contribution, which vanishes in the clean limit for $\mu = 0$ is now non-vanishing, though small, as a result of the impurity-induced smearing on a frequency scale $1/\tau$, as may be seen from the plot of thermal conductivity vs. frequency in Fig. 4

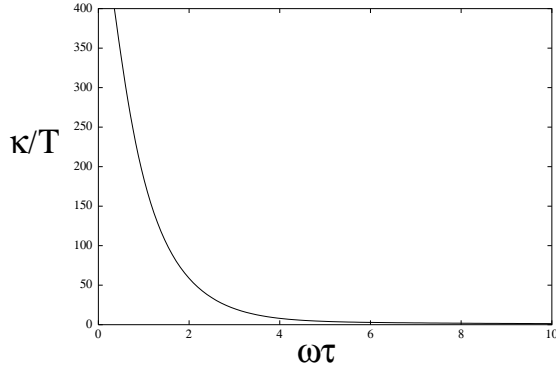


FIG. 4. The frequency-dependent thermal conductivity of the DDW state in the impurity-scattering-dominated limit. The thermal conductivity divided by T is in units of $8/e^2\alpha$ while the scale for $\omega\tau$ is 10^{-1} .

The contrast between Figs. 3 and 4 summarizes the distinction between the electrical and thermal conductivities of DDW nodal quasiparticles. In the case of the DSC state, there is no such contrast.

The basic fact which we uncovered in the $\tau = \infty$ limit still holds: nodal quasiparticles in the DDW state are qualitatively better carriers of electrical current than thermal current while nodal quasiparticles in the DSC state exhibit no such dichotomy.

As in the clean case, the electrical conductivity in a state with both DDW and DSC order follows the DDW case, with both a Drude and an Interband part. The main difference is the modified α of (55). The thermal conductivity is the same as in either the DDW or DSC states, but with the velocities combined as in (56).

VI. ELECTRICAL AND THERMAL HALL CONDUCTIVITIES

We now consider transport in a magnetic field. For weak magnetic fields, we would, in general, expect $\sigma_{xy}, \kappa_{xy} \propto B$ purely on symmetry grounds. A direct calculation shows that in the DDW state,

$$\sigma_{xy} = 16e^3 B \tau^2 v_F v_{\Delta}^{\text{DDW}} \quad (61)$$

$$\kappa_{xy} = \frac{16\pi^2}{3} e B \tau^2 T v_F v_{\Delta}^{\text{DDW}} \quad (62)$$

Note that this result holds for finite μ : the μ dependence of the hole density, $|\mu|$, cancels the μ dependence of the cyclotron frequency, $ev_F v_{\Delta}^{\text{DDW}}/|\mu|$. Hence, the Hall constant is

$$R_H = \frac{256}{\pi^2} \frac{v_F v_{\Delta}^{\text{DDW}}}{\alpha^2} \min\left(\frac{1}{|\mu|^2}, \tau^2\right) \quad (63)$$

The effective carrier concentration measured by R_H varies as μ^2 – not as μ – as a result of the peculiar μ -independence of σ_{xy} . Keep in mind, however, that these

results are strictly for the regime in which transport is dominated by nodal quasiparticles.

The large B limit can be understood by considering the effect of a magnetic field on nodal quasiparticles in the clean limit. Nodal quasiparticles satisfy the equation

$$\left[\sigma_{AB}^{(3)} v_F (i\partial_x + eA_x) + \sigma_{AB}^{(1)} v_{\Delta} (i\partial_y + eA_y) \right] \chi_{\alpha A} = E \chi_{\alpha A} \quad (64)$$

Squaring the differential operator which acts on χ , we have:

$$\left[v_F^2 (i\partial_x + eA_x)^2 + v_{\Delta}^2 (i\partial_y + eA_y)^2 + \sigma^{(2)} v_F v_{\Delta} eB \right] \chi = E^2 \chi \quad (65)$$

The solutions of this equation form Landau levels at energies

$$E_n = \pm \sqrt{v_F v_{\Delta} eB n} \quad (66)$$

for $n = 0, 1, \dots$. For $\omega_c \tau \gg 1$, these will give quantized Hall conductances.

By way of contrast, consider the linear response calculation in the DSC state and in the state with DDW and DSC order

$$\begin{aligned} \Pi_3^{CCC}(i\omega_n \rightarrow \omega + i\delta, \mathbf{q}, T) &= 0 \\ \Pi_3^{EEC}(i\omega_n \rightarrow \omega + i\delta, \mathbf{q}, T) &= 0 \end{aligned} \quad (67)$$

Consequently, the electrical and thermal Hall conductivities vanish in these states *at the level of approximation used in this paper*, namely linearization about the Fermi surface. In fact, they vanish *a fortiori* in this approximation, since the quasiparticles in a superconducting state do not couple to the electromagnetic field \mathbf{A} alone, but to the supercurrent $\nabla\varphi - \mathbf{A}$, so that these response functions must be multiplied by the curl of the supercurrent – which oscillates about zero mean in the vortex lattice state – not the magnetic field.

A number of authors have shown that non-zero Hall conductivities are obtained in the superconducting state only when one takes into account corrections to the linearization about the nodes. This is discussed thoroughly elsewhere, so we will not dwell on it here, and will limit ourselves to the observation that the situation in the DDW state is very different from that in the DSC state. According to the scaling laws discussed in [20–22], in the DSC state

$$\kappa_{xy} \sim T\sqrt{B} \quad (68)$$

Furthermore, the nodal quasiparticles of the DSC state do not form Landau levels but, rather, Bloch waves in the periodic potential caused by the supercurrent [23].

VII. DISCUSSION

Nodal quasiparticles are created equal, but some are more equal than others. The nodal quasiparticles of the DDW state are clearly different from those of the DSC state. The differences are a reflection of the symmetries which are broken in the two states. Broken translational symmetry in the DDW state leads to the existence of an Interband component of the electrical conductivity. This is a manifestation of the fact that quasiparticles and quasiholes in the DDW state can be visualized as electrons and positrons. A quasiparticle and quasihole with equal and opposite momenta carry twice the electrical current carried by either one of them and, at $\mu = 0$, zero energy current. These properties of DDW quasiparticles follow from the translational and rotational symmetry of the state, so they also apply to quasiparticles in graphite, in some models of quantum critical points [24], and in multi-band models [25].

This divergence between electrical and thermal transport is reminiscent of that observed in the experiments of [32], where $\kappa/\sigma T$ is found vanish at low temperatures in $\text{Pr}_{2-x}\text{Ce}_x\text{CuO}_4$ at magnetic fields greater than the upper critical field – i.e. in the presumed low-temperature ‘normal state’ with superconductivity suppressed. Such a severe violation only occurs in the DDW state in the extreme limit $\mu = 0$, $\tau = \infty$, as may be seen from (45) and (48). Nevertheless, it is interesting that such a counter-intuitive violation is possible at all.

There is no Interband component in the DSC state since it does not break translational symmetry. The DSC state has vanishing electrical and thermal Hall conductivities at the linear response level because $U(1)$ gauge symmetry is broken to Z_2 by the condensation of a charge- $2e$ order parameter. A DSC quasiparticle is a mixture of an electron and a hole, which should not have a Hall effect. Quasiparticles of the DSC state are essentially superpositions of particle and hole excitations of an ordinary Fermi surface, and they inherit the familiar properties of such excitations: they carry $\pi^2 T/3$ units of energy for each unit e of charge. (However, in any superconductor, the condensate carries electrical current but no thermal current, again violating the Wiedemann-Franz law.)

At present, there is insufficient experimental data on clean, highly-underdoped cuprates with a well-developed pseudogap to make a comparison with our results. This is the relevant limit because our calculations are applicable to the regime in which transport is dominated by quasiparticles which are close enough to the nodal points $(\pm \frac{\pi}{2a}, \pm \frac{\pi}{2a})$ that we can safely consider only linear order in deviations of the momentum about these points. In other words, our results apply to small values of the chemical potential μ . They would certainly apply to a putative DDW state very close to half-filling, but DDW order is unlikely to occur very close to half-filling since an-

tiferromagnetism is the predominant ordering tendency there. At the more significant doping levels at which superconductivity occurs, we might worry that the approximations used in this paper will no longer apply to the DDW state. However, there are several reasons why we believe that these fears may be misplaced. Angle-resolved photoemission experiments find a Fermi surface which has not moved very far along the Brillouin zone diagonals from $(\pm \frac{\pi}{2a}, \pm \frac{\pi}{2a})$ [5,6]. Even a naive determination of the Fermi surface, using the band structure of (3) and (4) with $t' = 0.45t$ finds small hole pockets about $(\pm \frac{\pi}{2a}, \pm \frac{\pi}{2a})$. Furthermore, measurements of the chemical potential [26] find that $\mu \propto x^2$ rather than the naively-expected dependence $\mu \propto x$; a similar result is found in Monte Carlo numerical studies of the 2D Hubbard model [27,28]. This could occur if the doped holes are confined to the boundaries between hole-poor regions [29,30], thereby pinning the chemical potential close to zero. Thus, our finite-frequency results, which are most interesting in the regime $\mu < \omega < \Delta_0$ may have a non-zero window of validity. We find it curious and possibly quite fortuitous that high quality YBCO crystals, which find evidence for DDW order, also exhibit the strongest evidence for dynamical stripes [31], which could pin the chemical potential at small values.

To summarize, we have, in this paper, shown how the differences between nodal quasiparticles in the DDW and DSC states can be probed by low-temperature transport measurements. The most notable signatures are the dichotomy between electrical and thermal transport and the existence of a linear in B Hall response in the DDW state – neither of which is a characteristic of nodal quasiparticles in the DSC state.

We would like to thank Sudip Chakravarty for discussions. This work was supported by the National Science Foundation under Grant No. DMR-9983544 and the A.P. Sloan Foundation.

APPENDIX A: KUBO FORMULAE

The Kubo formulae relate transport coefficients to retarded correlation functions of current operators. We will obtain the latter by analytic continuation of the imaginary-time correlation functions.

To this end, we define the Matsubara-frequency current-current correlation functions:

$$\begin{aligned} \Pi_2^{CC}(i\omega_n, \mathbf{q}, T) &= \int_0^\beta d\tau e^{i\omega_n\tau} \langle T_\tau j_x(\mathbf{q}, \tau) j_x(-\mathbf{q}, 0) \rangle \\ \Pi_2^{EE}(i\omega_n, \mathbf{q}, T) &= \int_0^\beta d\tau e^{i\omega_n\tau} \langle T_\tau j_x^E(\mathbf{q}, \tau) j_x^E(-\mathbf{q}, 0) \rangle \\ \Pi_2^{EC}(i\omega_n, \mathbf{q}, T) &= \int_0^\beta d\tau e^{i\omega_n\tau} \langle T_\tau j_x^E(\mathbf{q}, \tau) j_x(-\mathbf{q}, 0) \rangle \end{aligned} \quad (\text{A1})$$

and three-current correlation functions:

$$\begin{aligned}
\Pi_3^{CCC}(i\omega_n, \mathbf{q}, T) &= \int_0^\beta d\tau d\tau' e^{i\omega_n\tau} \langle T_\tau j_y(\mathbf{q}, \tau) j_x(0, 0) j_y(-\mathbf{q}, \tau') \rangle \\
\Pi_3^{ECC}(i\omega_n, \mathbf{q}, T) &= \int_0^\beta d\tau d\tau' e^{i\omega_n\tau} \langle T_\tau j_y^E(\mathbf{q}, \tau) j_x(0, 0) j_y(-\mathbf{q}, \tau') \rangle \\
\Pi_3^{EEC}(i\omega_n, \mathbf{q}, T) &= \int_0^\beta d\tau d\tau' e^{i\omega_n\tau} \langle T_\tau j_y^E(\mathbf{q}, \tau) j_x^E(0, 0) j_y(-\mathbf{q}, \tau') \rangle \quad (\text{A2})
\end{aligned}$$

The frequency-dependent electrical conductivity is given by the Kubo formula

$$\sigma_{xx}(\omega, T) = \frac{1}{\omega} \text{Im} \left\{ \Pi_2^{CC}(i\omega_n \rightarrow \omega + i\delta, 0, T) \right\} \quad (\text{A3})$$

Meanwhile, the Hall conductivity is obtained from a correlation function of three currents,

$$\sigma_{xy}(\omega, T)/B = \frac{1}{\omega} \frac{1}{q_x} \text{Im} \left\{ \Pi_3^{CCC}(i\omega_n \rightarrow \omega + i\delta, \mathbf{q} \rightarrow 0, T) \right\} \quad (\text{A4})$$

The thermal conductivity is given by the the following combination of correlation functions

$$\kappa_{xx}(\omega, T) = \frac{1}{T} \frac{1}{\omega} \text{Im} \left\{ \Pi_2^{EE}(i\omega_n \rightarrow \omega + i\delta, 0, T) \right\} - T S^2(\omega, T) \sigma_{xx}(\omega, T) \quad (\text{A5})$$

The second term on the right-hand-side ensures that the energy current flows under a condition of vanishing electrical current. It involves the thermopower, $S(\omega, T)$:

$$S(\omega, T) = - \frac{1}{T} \frac{\text{Im} \left\{ \Pi_2^{EC}(i\omega_n \rightarrow \omega + i\delta, 0, T) \right\}}{\text{Im} \left\{ \Pi_2^{CC}(i\omega_n \rightarrow \omega + i\delta, 0, T) \right\}} \quad (\text{A6})$$

The thermal Hall conductivity is given by

$$\kappa_{xy}(\omega, T)/B = \frac{1}{T} \frac{1}{\omega} \frac{1}{q_x} \text{Im} \left\{ \Pi_3^{EEC}(i\omega_n \rightarrow \omega + i\delta, \mathbf{q} \rightarrow 0, T) \right\} - T N^2(\omega, T) \sigma_{xy}(\omega, T) \quad (\text{A7})$$

where $N(\omega, T)$ is the Nernst coefficient, or Hall thermopower:

$$N(\omega, T)/B = \frac{1}{T} \frac{\text{Im} \left\{ \Pi_2^{ECC}(i\omega_n \rightarrow \omega + i\delta, \mathbf{q} \rightarrow 0, T) \right\}}{\text{Im} \left\{ \Pi_2^{CCC}(i\omega_n \rightarrow \omega + i\delta, \mathbf{q} \rightarrow 0, T) \right\}} \quad (\text{A8})$$

APPENDIX B: IMPURITY SCATTERING OF NODAL QUASIPARTICLES

We briefly review the effect of impurity scattering on nodal quasiparticles. Let us assume that the impurities

can be described by a δ -function-correlated, Gaussian-distributed random potential with variance V_0 :

$$\overline{V(\mathbf{x})V(\mathbf{x}')} = |V_0|^2 \delta^{(2)}(\mathbf{x} - \mathbf{x}') \quad (\text{B1})$$

Consider the graph in figure (5) which determines the quasiparticle self-energy to lowest order. For nodal quasiparticles, both the real and imaginary parts are logarithmically divergent in the infrared. Hence, we compute the self-energy self-consistently

$$\Sigma^1(i\epsilon_n) = \frac{|V_0|^2}{v_F v_\Delta} \int \frac{d^2k}{(2\pi)^2} \frac{i\epsilon_n + \Sigma(i\epsilon_n) + \sigma \cdot \mathbf{k}}{(\epsilon_n + i\Sigma^1(i\epsilon_n))^2 + k^2} \quad (\text{B2})$$

A similar expression holds for the self-energy for the other pair of nodes, $\Sigma^2(i\epsilon_n)$. In this expression, we have rescaled k_x, k_y to remove the velocities from the Green function and bring them outside the integral. Solving this equation self-consistently, we find $\Sigma^1(i\epsilon_n \rightarrow 0) = i/2\tau \text{sgn}(\epsilon_n)$ with

$$\tau = \frac{1}{\Lambda} e^{2\pi v_F v_\Delta / |V_0|^2} \quad (\text{B3})$$

where Λ is the ultraviolet cutoff on the nodal effective Lagrangian. This effective theory certainly breaks down at scales comparable to the maximum of the gap, so we should take $\Lambda \lesssim \Delta_0$. Meanwhile,

$$\text{Re}\Sigma^1(i\epsilon_n \rightarrow 0) = \left[\frac{\frac{|V_0|^2}{2\pi v_F v_\Delta} \ln(2\Lambda\tau)}{1 - \frac{|V_0|^2}{2\pi v_F v_\Delta} \ln(2\Lambda\tau)} \right] i\epsilon_n \quad (\text{B4})$$

This can be absorbed into a redefinition of the velocities.

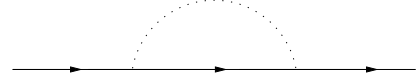


FIG. 5. The leading diagram which contributes to the quasiparticle self-energy.

Hence, the Green function in the presence of impurities is:

$$G^1(i\epsilon_n, \mathbf{k}) = \frac{i\epsilon_n + i/2\tau \text{sgn}(\epsilon_n) + \sigma \cdot \mathbf{k}}{(i\epsilon_n + i/2\tau \text{sgn}(\epsilon_n))^2 - k^2} \quad (\text{B5})$$

where the momenta have been rescaled so that $k^2 = v_F^2 k_x^2 + v_\Delta^2 k_y^2$ and $\mathbf{k} = (v_F k_x, v_\Delta k_y)$ on the right-hand-side of (B5).

This result holds for the DDW state at $\mu = 0$ or the DSC state for arbitrary μ . In the former case, the matrix indices correspond to momenta \mathbf{k} and $\mathbf{k} + \mathbf{Q}$; in the latter case, they are particle/hole indices. The associated matrix spectral function $A(k, 0)$ is

$$A^1(\epsilon, \mathbf{k}) = \frac{1}{2\pi\tau} \frac{\epsilon^2 + k^2 + 1/(2\tau)^2 + 2\epsilon\sigma \cdot \mathbf{k}}{[(\epsilon + k)^2 + 1/(2\tau)^2][(\epsilon - k)^2 + 1/(2\tau)^2]} \quad (\text{B6})$$

For the DDW state at non-zero μ , we have

$$A^1(\epsilon, \mathbf{k}) = \frac{1}{2\pi\tau} \frac{(\epsilon + \mu)^2 + k^2 + 1/(2\tau)^2 + 2(\epsilon + \mu)\sigma \cdot \mathbf{k}}{[(\epsilon + \mu + k)^2 + 1/(2\tau)^2][(\epsilon + \mu - k)^2 + 1/(2\tau)^2]} \quad (\text{B7})$$

with similar expressions for $A^2(\epsilon, \mathbf{k})$.

These spectral functions are used in the calculations in sections VI and VII.

Dai, H. A. Mook, R. D. Hunt, and F. Dogan, Phys. Rev. B **63**, 54525 (2001).

[32] R.W. Hill, *et al.*, unpublished.

-
- [1] For reviews, see *Physical Properties of High Temperature Superconductors*, Edited by D. M. Ginsberg (World Scientific, Singapore) Vol. I (1989), Vol. II (1990), Vol. II (1992), Vol. IV (1994).
- [2] S. Chakravarty, R. B. Laughlin, D. K. Morr, C. Nayak, Phys. Rev. B **63**, 94503 (2001).
- [3] T. Timusk and B. Statt, Rep. Prog. Phys. **62**, 61 (1999).
- [4] C. Nayak, Phys. Rev. B **62**, 4880 (2000).
- [5] M. R. Norman *et al.*, Nature **392**, 157(1998).
- [6] J. M. Harris, *et al.*, Phys. Rev. B **54**, R15665 (1996).
- [7] Ch. Renner *et al.*, Phys. Rev. Lett. **80**, 149(1998).
- [8] H. F. Fong, *et al.*, Phys. Rev. B **61**, 14773 (2000).
- [9] P. Dai, *et al.*, Science **284**, 1344 (1999).
- [10] C. C. Homes, *et al.*, Phys. Rev. Lett. **71**, 1645 (1993).
- [11] J. L. Tallon *et al.*, Phys. Stat. Sol. B **215**, 531 (1999); J. W. Loram *et al.*, J. Phys. Chem. Solids **59**, 2091 (1998).
- [12] G. Bilbro and W. L. McMillan, Phys. Rev. B **14**, 1887 (1976).
- [13] V. Vescoli, *et al.*, Phys. Rev. Lett. **81**, 453 (1998).
- [14] A. H. Castro Neto, cond-mat/0012147.
- [15] H. A. Mook, P. Dai, F. Dogan, Phys. Rev. B **64**, 012502 (2001); H. A. Mook, *et al.*, unpublished.
- [16] J. E. Sonier, *et al.*, Science **292**, 1692 (2001).
- [17] C. Nayak, *et al.*, cond-mat/0105357.
- [18] D. J. Scalapino, S. R. White, and S. C. Zhang, Phys. Rev. Lett. **68**, 2830 (1992).
- [19] A.-M. Tremblay, *et al.*, Phys. Rev. A **19**, 1721 (1979).
- [20] S. H. Simon and P.A. Lee, Phys. Rev. Lett. **78**, 1548 (1997).
- [21] J. Ye, Phys. Rev. Lett. **86**, 316 (2001).
- [22] O. Vafek, *et al.*, cond-mat/0104516.
- [23] M. Franz and Z. Tesanovic, Phys. Rev. Lett, **83**, 554 (2000).
- [24] A. Ludwig, M. P. A. Fisher, R. Shankar, and G. Grinstein, Phys. Rev. B **50**, 7526 (1994).
- [25] C. M. Varma, Phys. Rev. Lett. **83**, 3538 (1999).
- [26] A. Ino *et al.*, Phys. Rev. Lett, **79**, 2101 (1997).
- [27] E. Dagotto *et al.*, Phys. Rev. Lett, **67**, 1918 (1991).
- [28] N. Furukawa and M. Imada, J. Phys. Soc. Jpn. **62**, 2557 (1993).
- [29] J. Zaanen and A. M. Olé, Ann. Phys. (Leipzig) **5**, 224 (1996).
- [30] V. J. Emery, S. A. Kivelson, and O. Zachar, Phys. Rev. B, **56**, 6120, (1997).
- [31] H. A. Mook and F. Dogan, Nature **401**, 145 (1999); P.